

## Evaporation and Precipitation Surface Effects in Local Mass Continuity Laws of Moist Air

ULRIKE WACKER

*Alfred-Wegener-Institut für Polar- und Meeresforschung, Bremerhaven, Germany*

THOMAS FRISIUS AND FRITZ HERBERT

*Theoretische Meteorologie, J. W. Goethe-Universität Frankfurt am Main, Frankfurt am Main, Germany*

(Manuscript received 3 August 2004, in final form 13 January 2006)

### ABSTRACT

The local mass balance equations of cloudy air are formulated for a model system composed of dry air, water vapor, and four categories of water condensate particles, as typically adopted for numerical weather prediction and climate models. The choice of the barycentric velocity as reference motion provides the most convenient form of the total mass continuity equation. Mass transfer across the earth's surface due to precipitation and evaporation causes a nonvanishing barycentric vertical velocity  $w_s$ , and is proportional to the local difference between evaporation rate and rain plus snow rate. Hence  $w_s$  vanishes only in the special situation that evaporation and precipitation balance exactly. Alternative concepts related to different reference motions are reviewed. However, the choice of the barycentric velocity turns out to be advantageous for several reasons.

The implication of the nonvanishing total mass transport across the earth's surface is estimated from model simulations for two extreme weather situations: a polar cold air outbreak and a tropical cyclone. While the effect is small in the first case, it is important in the latter. The large precipitation rates in the tropical cyclone case cause a loss of atmospheric mass, which corresponds to a vertical velocity at the surface larger than  $-20 \text{ mm s}^{-1}$ , and an instantaneous drop in pressure, which if sustained for 6 h, would correspond to about 49 hPa; this demonstrates the necessity of using the correct formulation of the mass balance in simulation models for moist air.

### 1. Introduction

The mathematical simulation of the evolution of cloudy air requires the treatment of the gas with suspended liquid and ice particles as a multicomponent and multiphase system. While each constituent moves at its own velocity, the mixture as a whole moves at its barycentric (mean mass weighted) velocity. The difference in velocities of the mixture and its constituents becomes evident for, most notably, precipitating elements that fall at a speed of up to several meters per second relative to their ambient air. Precipitation transports mass from the atmosphere to the surface, whereby not only the mass budget of the condensate is

affected, but also the mass budget of the air mixture. Therefore, an appropriate reference velocity should be chosen to which the relative transport velocities (diffusion velocities) of the system's constituents can be referred.

The scientific discussion of how appropriately to formulate the fundamental set of thermo-hydrodynamic equations for cloudy air has come up again recently, mostly in connection with the design and development of a new generation of simulation models for the purpose of climate research and numerical weather prediction (NWP). Examples are presented by Satoh (2003) for a Japanese cloud ensemble model, Saito (1998) for the Japanese mesoscale NWP model, Ooyama (2001) and Bannon (2002) for models of moist convection, and L. Bonaventura et al. (2003, personal communication) for the design of the new German Icosahedral Nonhydrostatic General Circulation Model (ICON GCM). One basic problem is the choice of the reference veloc-

---

*Corresponding author address:* Dr. Ulrike Wacker, Alfred-Wegener-Institut für Polar- und Meeresforschung in der Helmholtz-Gemeinschaft, Bussestr. 24, 27515 Bremerhaven, Germany.  
E-mail: uwacker@awi-bremerhaven.de

ity. However, in most of the papers mentioned, a proper discussion of the choice of the reference velocity and related consequences to, for example, the mass budget equations is missing.

In the case of cloudy air, some candidates for the reference velocity are 1) the barycentric velocity of all contributing substances, dry air + water vapor + water condensate, known as the total system, 2) merely the barycentric velocity of the gas mixture consisting of dry air + water vapor, or 3) just the dry air component velocity. It should not surprise that the proposed formulations of the set of the thermo-hydrodynamic equations, although they express the same physical facts, differ when different reference velocities are used.

Treatises on the reference velocity in general and implications of various specifications are given by, for example, Gyarmati (1970), Haase (1990), and Herbert (1983). More recently, Wacker and Herbert (2003), hereafter referred to as WH03, have formulated the mass continuity equations for various reference velocities applying to a three constituent substance consisting of dry air, water vapor, and water condensate particles (liquid water drops or ice particles). Although no contradiction is involved in the use of one of the alternative set of equations, it was nevertheless recommended to use the barycentric velocity of the cloudy air mixture as the reference velocity, since that frame allows a particularly convenient and transparent formal representation of all the field equations of continuity. However, in WH03, no distinction was made between liquid water and ice as well as between airborne cloud particles and precipitating particles.

A precise mass balance also requires correct boundary conditions, which in turn depend on the chosen reference frame for velocity. With regard to the velocity perpendicular to the earth's surface; that is, its vertical component in case of a flat surface, the lower boundary conditions for each of the relevant velocities were provided in WH03. Mass transports of dry air across the surface result, for example, from emission of CO<sub>2</sub>, exhalation of trace gases, and the whirling up of dust. They may become locally important for the total mass budget, and they can be accounted for in a similar way as the mass fluxes of water. On a larger scale, however, their contribution is small. Therefore, they are disregarded in this paper, and the surface is assumed impenetrable to dry air. Thus the dry air velocity perpendicular to the surface vanishes, that is in case of a flat surface

$$w_{ds} = 0, \quad (1)$$

with  $w_d$  denoting the vertical velocity of dry air and with index  $s$  denoting the surface. The barycentric ver-

tical velocity, however, does not generally vanish at a flat surface, but must account for any net mass transport due to precipitation and evaporation. According to WH03, barycentric vertical velocity is proportional to the total mass flux across the surface due to evaporation and precipitation. Likewise, sea spray formation signifies a further mass transport into the atmosphere; owing to the rapid sedimentation of large spray drops (Andreas 2004), the net water mass transport is not regarded here.

A change of mass due to evaporation and precipitation across the boundary is related to surface pressure changes, as pointed out by Trenberth (1991), Trenberth et al. (1995), Lackmann and Yablonsky (2004), and WH03. This effect should be accounted for in the surface pressure tendency equation. Indeed, Lackmann and Yablonsky (2004) report from hurricane simulations with the hydrostatic NCEP Eta model that atmospheric mass removal via precipitation exerts a nonnegligible influence on the dynamics of the tropical cyclone. Moreover, Trenberth (1991) as well as Lackmann and Yablonsky (2004) suggest that the continuity equation in pressure coordinates should comprise evaporation and precipitation source as well as sink terms. Whether such contributions should be considered or not depends on the mass density employed (i.e., density of total system, of gas mixture, or of dry air) and on the reference velocity employed, as discussed in section 3.

The first aim of this study is to formulate for each of the partial masses and for total mass the continuity equations for application in, for example, numerical weather prediction models and climate models. Since parameterization schemes applied in contemporary weather forecast and climate models often account for the effects of cloud microphysical processes, the concept discussed in WH03 is extended here by subdividing the water condensate particle category into several categories: cloud water drops, cloud ice crystals, rain drops, and precipitating ice particles (e.g., snowflakes and graupel). In agreement with such descriptions, we assume cloud water droplets and cloud ice crystals to be sufficiently small to neglect their sedimentation. For this system we derive in section 2 general relationships for the mass balance equations. We assume the barycentric velocity of the full air mixture as the reference frame and formulate the continuity equations for partial masses and total mass. Then, we derive the matching boundary condition for the velocity perpendicular to the earth's surface and the surface pressure tendency equation. This is supplemented in section 3 by a review of alternative concepts in the literature.

The second aim of the study is to estimate the sig-

nificance of the net mass fluxes across the surface due to evaporation and precipitation; this is presented in section 4. Lacking a numerical model that fully accounts for the correct lower boundary conditions, we diagnose the barycentric vertical velocity  $w_s$  and corresponding surface pressure tendencies from the surface evaporation rate and the surface precipitation rate as simulated by the mesoscale operational weather prediction model Lokal-Modell (LM) of the Deutscher Wetterdienst (DWD; Doms and Schättler 1999, 2002; Steppler et al. 2003). Since meteorological conditions can be highly variable over the globe, we will look at the surface mass fluxes for two extreme weather situations: 1) a polar cold air outbreak (section 4a) and 2) a tropical cyclone (section 4b).

## 2. The mass balance model in the reference frame of the barycentric velocity

### a. The mass continuity equations in a general reference frame

The conceptual atmospheric model we consider is a diluted heterogeneous mixture consisting of dry air and water vapor as homogeneous gaseous components as well as liquid and solid water in several particle forms such as cloud drops, cloud ice particles, precipitating drops (rain), and precipitating ice particles (snow, graupel, etc.). In the following, each of these six constituents is indicated by the subscripts  $k = d, v, w, i, r, p$ , respectively. We will loosely refer to the particle categories as components like the gaseous components. Furthermore, dry air is treated as a chemically inert gas. As a measure for any component concentration we use the partial density  $\rho_k$ . The total density  $\rho$  of the mixture is then

$$\rho = \sum_k \rho_k = \rho_d + \rho_v + \rho_w + \rho_i + \rho_r + \rho_p. \quad (2)$$

In equivalence with the global integral mass balance criterion of a component  $k$ , one can set up corresponding local balance differential equations, henceforth referred to as (mass) continuity equations,

$$\frac{\partial \rho_k}{\partial t} = -\nabla \cdot \mathbf{F}_k + \sigma_k, \quad \text{with } k = d, v, w, i, r, p. \quad (3)$$

In (3) the vector  $\mathbf{F}_k$  denotes the divergent mass flux density of component  $k$ ; by definition

$$\mathbf{F}_k = \rho_k \mathbf{v}_k, \quad (4)$$

wherein the transport velocity vector  $\mathbf{v}_k$  is the velocity of component  $k$ . The second term  $\sigma_k$  on the right-hand side of (3) is the internal source strength rate. The con-

dition of conservation of total mass means that the sum of all  $\sigma_k$  source strength terms vanishes,

$$\sum_k \sigma_k = \sigma_d + \sigma_v + \sigma_w + \sigma_i + \sigma_r + \sigma_p = 0. \quad (5)$$

The component velocities  $\mathbf{v}_k$  are all different in general. Hence we observe not only a macroscopic motion with a certain reference velocity  $\mathbf{v}_{\text{ref}}$ , which is to be specified, but also a motion of each component relative to  $\mathbf{v}_{\text{ref}}$  represented by the diffusion velocity  $\mathbf{v}'_k = \mathbf{v}_k - \mathbf{v}_{\text{ref}}$ . The mass flux vector  $\mathbf{F}_k$  as defined in (4) may be split into a contribution due to the macroscopic reference motion and a contribution due to the diffusive motion:

$$\mathbf{F}_k = \rho_k \mathbf{v}_{\text{ref}} + \rho_k \mathbf{v}'_k = \rho_k \mathbf{v}_{\text{ref}} + \mathbf{J}_{\text{ref},k}, \quad (6)$$

where  $\mathbf{J}_{\text{ref},k} = \rho_k \mathbf{v}'_k$  is introduced as the diffusion mass flux relative to any reference velocity.

The continuity equation of total mass follows from Eqs. (2), (3), (5), and (6) as

$$\frac{\partial \rho}{\partial t} + \nabla \cdot (\rho \mathbf{v}_{\text{ref}}) = -\sum_k \nabla \cdot \mathbf{J}_{\text{ref},k}. \quad (7)$$

### b. The mass continuity equations in the barycentric reference frame

In geophysical fluid dynamics, the barycentric velocity (i.e., the mean mass weighted velocity of the system) is frequently chosen as the reference velocity. For our basic system this velocity is given by

$$\mathbf{v} = \frac{\rho_d \mathbf{v}_d + \rho_v \mathbf{v}_v + \rho_w \mathbf{v}_w + \rho_i \mathbf{v}_i + \rho_r \mathbf{v}_r + \rho_p \mathbf{v}_p}{\rho}, \quad (8)$$

where each fraction  $\rho_k/\rho$  denotes a weighting factor. With (6) and (8) the continuity equation (3) for a component  $k$  transforms to

$$\frac{\partial \rho_k}{\partial t} = -\nabla \cdot (\rho_k \mathbf{v} + \mathbf{J}_k) + \sigma_k \quad \text{for } k = d, v, w, i, r, p. \quad (9)$$

In (9)  $\rho_k \mathbf{v}$  denotes the advective mass flux of component  $k$  in the barycentric reference frame. From the definition of the  $\mathbf{J}_k$  fluxes as  $\mathbf{J}_k = \rho_k (\mathbf{v}_k - \mathbf{v})$ , it follows that their sum is zero:

$$\mathbf{J}_d + \mathbf{J}_v + \mathbf{J}_w + \mathbf{J}_i + \mathbf{J}_r + \mathbf{J}_p = 0. \quad (10)$$

If we account for a turbulent medium and interpret  $\rho_k$ ,  $\mathbf{v}$ ,  $\mathbf{J}_k$ , and  $\sigma_k$  as ensemble averaged values, the local mass balance equation reads

$$\frac{\partial \rho_k}{\partial t} = -\nabla \cdot (\rho_k \mathbf{v} + \mathbf{J}_k + \mathbf{F}_k^T) + \sigma_k \quad \text{for } k = d, v, w, i, r, p, \quad (11)$$

wherein  $\mathbf{F}_k^T$  denotes the partial turbulent mass flux. Adopting the mass weighted averaging technique according to Hesselberg (1926) to yield (11), then the sum of the  $\mathbf{F}_k^T$  vanishes:

$$\mathbf{F}_d^T + \mathbf{F}_v^T + \mathbf{F}_w^T + \mathbf{F}_i^T + \mathbf{F}_r^T + \mathbf{F}_p^T = 0. \quad (12)$$

For inert dry air, the source rate vanishes,  $\sigma_d = 0$ . For the water categories, the source terms account for mass interactions due to phase changes as well as coagulation processes. Such mass transformations may be determined on the basis of a detailed treatment of cloud microphysics (which is numerically very expensive) or on the basis of a corresponding parameterization model.

Summing Eqs. (9) or Eqs. (11) over all components  $k = d, v, w, i, r, p$ , and regarding the mass control conditions (5), (10), and (12), the familiar total mass continuity equation follows as

$$\frac{\partial \rho}{\partial t} = -\nabla \cdot (\rho \mathbf{v}). \quad (13)$$

In the molecular sublayer, molecular diffusion causes the vertical transport of water vapor between the surface and the lowest millimeters of air. Beyond the lowest few centimeters, turbulent transport dominates over molecular transport (Stull 1994). Nevertheless, we retain the divergence of the molecular vertical diffusion fluxes, despite being small only few centimeters beyond the very thin molecular layer, for the following reason: Water vapor can enter the atmosphere at the earth's surface due to evaporation and sublimation or leave the atmosphere due to formation of dew and frost. This means a mass transport into/out of the materially open system atmosphere; all these processes will be summarized henceforth as evaporation for simplicity.

Since in this context we will only consider relations for the vertical  $\mathbf{J}_k$  flux components, these are simply denoted as  $J_k$  as well as their surface boundary values as  $J_{ks}$ . So, for instance,  $J_{vs} = \rho_{vs}(w_{vs} - w_s)$  expresses the upward directed component of the molecular vapor diffusion flux at the surface. In this  $J_{vs}$  formula the velocity  $w_{vs}$ , in difference to the vanishing  $w_{ds}$  subject to boundary condition (1), is prerequisite for the supply of water vapor into the air. To emphasize this point, we will not include  $\mathbf{J}_k$  in  $\mathbf{F}_k^T$  because the turbulent flux occurs also if one has  $w_v = w_d$ .

The component velocities of the populations of rain drops and precipitating ice particles,  $\mathbf{v}_r$  and  $\mathbf{v}_p$  are interpreted as the mean mass weighted velocity of the respective populations. The vertical components of the diffusion velocities  $\mathbf{v}'_r$  and  $\mathbf{v}'_p$  are approximated by the so-called sedimentation or terminal fall velocity as

given, for example, in the treatise of Rogers and Yau (1989). Therefore, the vertical components of the flux vectors  $\mathbf{J}_r$  and  $\mathbf{J}_p$  denoted as  $J_r$  and  $J_p$ , can be approximated by the downward directed sedimentation fluxes  $S_r$  and  $S_p$ , henceforth referred to as the sedimentation (or simply precipitation) rates:

$$S_r = -J_r, \quad S_p = -J_p. \quad (14)$$

With (14) we do not imply turbulent transport of precipitating particles as well as all horizontal diffusion fluxes; such effects are disregarded.

It is also to notify that, different from our representation of the surface diffusion fluxes of water vapor and precipitating particles in terms of  $J_{vs}$  and  $S_s$ , respectively, other studies, for example, Trenberth (1991), describe the total surface mass transfer in form of the surface evaporation rate

$$E = \rho_{vs} w_{vs} = \rho_{vs} w_s + J_{vs}, \quad (15)$$

and the surface precipitation rate

$$P_l = -\rho_{ls} w_s + S_{ls} \quad (l = r, p). \quad (16)$$

Obviously, the two ways coincide for vanishing boundary reference velocity; in cases with  $w_s = 0$ , the two equalities  $E = J_{vs}$  and  $P_l = S_{ls}$  are valid.

With the above assumptions, the partial mass continuity equations read

$$\frac{\partial \rho_k}{\partial t} + \nabla \cdot (\rho_k \mathbf{v}) = -\frac{\partial J_k}{\partial z} - \nabla \cdot \mathbf{F}_k^T + \sigma_k \quad (17)$$

for the components dry air, water vapor, cloud water, and cloud ice ( $k = d, v, w, i$ ), as well as

$$\frac{\partial \rho_l}{\partial t} + \nabla \cdot (\rho_l \mathbf{v}) = \frac{\partial S_l}{\partial z} + \sigma_l \quad (18)$$

for the components rainwater and precipitating ice ( $l = r, p$ ).

### c. The surface boundary conditions

In this subsection, we will formulate the boundary conditions at the bottom of the atmosphere. For simplicity, we assume a flat earth surface. Of particular interest are the velocity and the partial mass fluxes perpendicular to the surface, that are the surface values of  $w, J_v, J_c, J_i, S_r$ , and  $S_p$ , respectively.

We have assumed, according to (1), that the earth's surface is impermeable to dry air. Evaporation and precipitation at the surface are connected evidently with nonzero values for the diffusion velocities,

$$w_{vs} \neq 0, \quad w_{rs} \neq 0, \quad w_{ps} \neq 0. \quad (19)$$

Moreover, the surface is assumed to be impermeable to cloud particles:

$$w_{ws} = 0, \quad w_{is} = 0. \quad (20)$$

Then we obtain from (8) considering (1), (19), (20), and the reformulations (14) the following expression for the barycentric boundary velocity  $w_s$  normally directed to the flat surface:

$$w_s = \frac{(\rho_v w_v)_s + (\rho_r w_r)_s + (\rho_p w_p)_s}{\rho_s} = \frac{E - P_r - P_p}{\rho_s} \quad (21)$$

$$= \frac{J_{us} - S_{rs} - S_{ps}}{(\rho_d + \rho_w + \rho_i)_s}. \quad (22)$$

Therefore, one can speak of a boundary condition  $w_s = 0$  only if evaporation and precipitation in the forms of rain and ice can be assumed to be in local balance. However, this is a rare situation in the natural atmosphere.

As an alternative, the diffusion fluxes could be assumed to vanish at the surface,  $J_{ws} = 0$  and  $J_{is} = 0$ , instead of (20). The resulting barycentric velocity  $w_s$  only differs from (22) by the denominator  $\rho_{ds}$  instead of  $(\rho_d + \rho_w + \rho_i)_s$ , and hence due to  $\rho_d \gg \rho_w, \rho_i$ , the difference is negligible.

A net gain or loss of mass of an air column changes the surface pressure  $p_s$ . With the continuity equation (13) and the assumption of locally hydrostatic density distribution over a flat boundary area,  $z_s = \text{const.}$ , one derives for the surface pressure  $p(z_s) = p_s$  the following tendency equation:

$$\frac{\partial p_s}{\partial t} = -g \int_{z_s}^{\infty} \nabla \cdot (\rho \mathbf{v}_h) dz + g[\rho w]_s. \quad (23)$$

In (23)  $\mathbf{v}_h$  represents the horizontal barycentric velocity and  $w_s$  the vertical barycentric velocity at the surface depending on evaporation and precipitation, see (21) or (22). Before (13) was integrated over  $z$  in order to yield (23), the  $\rho$  tendency term has been substituted in conjunction with the hydrostatic pressure gradient  $\partial p / \partial z = -\rho g$ ; therefore, the surface pressure tendency  $\partial p_s / \partial t$  is necessarily associated with the total mass density  $\rho$ . If  $w_s = 0$  is used as boundary condition, the effect of mass gain or loss due to evaporation and precipitation at the surface would not effect the  $p_s$  tendency.

Regardless of the choice of the reference velocity, the surface pressure is changed by the total vertical mass flux  $(\rho w)_s$  due to evaporation and precipitation,

see (21) or (22). Likewise, it is changed by the divergence of the horizontal mass flux  $\rho \mathbf{v}_h$ . If this flux is expressed in terms of the gas velocity  $\mathbf{v}_g$  or the dry air velocity  $\mathbf{v}_d$  instead of the barycentric velocity  $\mathbf{v}$ , then this total flux includes a contribution due to the reference motion and a contribution from related partial mass diffusion fluxes.

### 3. Alternative theoretical foundations

It is appropriate to this basic study to give a concise review of the theoretical framework used to select a reference velocity in other model studies, as well as the implications of the selection. Related to multicomponent fluid systems as, for example, treated in Gyarmati (1970) or Haase (1990), the barycentric velocity  $\mathbf{v}$  is adopted as the most suitable reference frame of motion. It represents the basic variable of the corresponding local momentum budget equation for the total system, referred to as Cauchy's equation of motion:

$$\rho \frac{d\mathbf{v}}{dt} = -\nabla \cdot \mathbf{P} + \rho \mathbf{F}. \quad (24)$$

In (24)  $\mathbf{P}$  denotes the full nonconvective momentum flux tensor (pressure tensor) and  $\rho \mathbf{F} = \sum \rho_k \mathbf{F}_k$  the vector sum of all external forces (per unit volume), which in the conceptual model presented here includes gravity and Coriolis forces. Gyarmati (1970) and Doms and Herbert (1985) discuss how to account for internal momentum transfers between the mass constituents in a multicomponent system such that (22) is not violated.

Ooyama (2001) considers the components dry air, water vapor, and cloud condensate, all of which float with the same velocity (hereafter named  $\mathbf{v}\{\text{Ooyama}\}$ ), and precipitation, which has an additional velocity contribution in the vertical. In that model the velocity  $\mathbf{v}\{\text{Ooyama}\}$  is chosen as the reference motion, and in consideration of this, the total mass continuity equation considers the deviation of the precipitation velocity. This author explicitly mentions the nonvanishing precipitation mass flux at the model surface. On the other hand, the model disregards evaporation at the earth's surface associated with the lower boundary condition  $w_s\{\text{Ooyama}\} = 0$ . Momentum budgets are formulated for  $\mathbf{v}\{\text{Ooyama}\}$  and for the precipitation velocity, wherein internal momentum sources due to interactions with other constituents are included. However, the associated total momentum equation does not take a form similar to (24), but contains a residual source term connected to phase changes. From that equation a slightly approximated version is derived as the final  $\mathbf{v}\{\text{Ooyama}\}$  equation.

In another study, Schubert et al. (2001) use a basic

concept akin to that of Ooyama (2001). As stated by the authors, the difference between the velocity of the constituents dry air, water vapor, and cloud condensate, and the barycentric velocity of the total system is very small in the atmosphere, so that a barely significant difference should result when  $\mathbf{v}$  in (24) is interpreted as any of those. However, one can see that matters become different close to the surface, where precipitation and evaporation dominate the value of the barycentric vertical velocity, see (22) for the boundary condition, while the dry air velocity tends to zero.

In passing we note that the calculation of the velocity of sedimenting condensate requires either knowledge of the pressure tensor and the relevant internal momentum transfer rates to solve the momentum equation for that constituent or other closure conditions. Mostly, the latter is preferred by replacing the equation of motion for sedimenting condensate by a diagnostic relation from which the unaccelerated (constant) terminal velocity is determined. Against Ooyama's (2001) reservations regarding such a procedure, it does not involve any systematic contradiction.

In his nonhydrostatic climate model Satoh (2003) closely follows the concept of Ooyama (2001) with regard to velocity, although allowing different partial velocities for all constituents. Nevertheless, the supply of water vapor from the ground is neglected in the model, hence, the vertical velocity of the airborne mixture vanishes at the surface. However, the outflow of precipitating mass at the surface is accounted for in the balance equations of the model.

As a basic postulate Bannon (2002) uses the velocity of dry air  $\mathbf{v}_d$  as reference motion. Hence, the lower boundary condition for the vertical velocity is straightforward  $w_{ds} = 0$  as in (1). It is assumed that dry air and water vapor move approximately with the same velocity, which would, in a strict sense, prevent any evaporation flux of vapor from the surface. Here  $\mathbf{v}_d$  follows from an equation of motion for the gas mixture. This equation contains contributions from the internal momentum transfer between the gas components and the condensate, for which the determination requires closure assumptions.

The vertical equation of motion according to (24) has the hydrostatic approximation  $0 = -\partial p/\partial z - g\rho$  where  $\rho$  is total density. If the hydrostatic approximation is applied to the momentum equations for the gas mixture of dry air alone, vertical pressure change is associated with the matching partial density. For instance, Trenberth (1991) and Trenberth et al. (1995) related the hydrostatic pressure to the density  $\rho_g$  of the gas mixture. The special form of the hydrostatic surface pressure tendency equation certainly depends on this

choice. Assuming again a flat surface, the resulting  $p_s$  equation of Trenberth is similar to (23) insofar as in both formulations the mass fluxes across the surface due to evaporation and precipitation contribute to the surface pressure tendency. Yet Trenberth's equations can be reproduced for a model with the condensate mass continuity equation replaced by a diagnostic equation stating the balance between the vertical divergence of the precipitation mass flux and the cloud physical conversion rates.

In this context, different versions of the continuity equation in pressure coordinates can be easily interpreted. Trenberth (1991) as well as, more recently, Lackmann and Yablonsky (2004), suggest that the common form

$$\nabla \cdot \mathbf{v}_h + \frac{\partial \omega}{\partial p} = 0, \quad (25)$$

with  $\mathbf{v}_h$  and  $\omega$  denoting the horizontal velocity vector and the vertical velocity in so-called pressure coordinates, respectively, should be supplemented by evaporation and precipitation source and sink terms. In view of our previous discussion of the mass continuity equation in different reference frames of velocity, the question whether (25) is complete can easily be answered; it depends on the choice of the reference velocity and on the interpretation of the density variable in the hydrostatic equation.

If the density variable is interpreted as the total density, and if the velocity variable is interpreted as the barycentric one  $\mathbf{v}$ , then the total mass continuity equation does not contain any source. This holds, in full equivalence, for the continuity equation in pressure coordinates. Hence, (25) represents the correct differential equation with respect to pressure coordinates. Evidently, the pressure velocity  $\omega$  is by definition  $\omega = dp/dt$  related to the barycentric velocity.

If the density variable in the hydrostatic equation is interpreted as merely dry air density, and if the velocity is interpreted likewise as that of dry air ( $\mathbf{v}_d$ ), then the continuity equation of dry air mass does not contain any source, and neither does the continuity equation in pressure coordinates. Hence, we find again the form (25), with the difference that  $\omega$  is now defined as  $\omega = d_d p/dt$ , where the total derivative  $d_d/dt$  includes the dry air velocity.

For any other interpretations of density and velocity variables, additional terms inevitably show up in the continuity equation because of phase changes and/or diffusion fluxes. For instance, if the density of the gas mixture and the velocity of dry air are employed, then the continuity equation comprises the rates of phase

changes between water vapor and condensate as well as the divergence of the water vapor diffusion flux. As an example, for model assumptions as used by Trenberth (1991), see above, and using the pressure velocity  $\omega = d_{\sigma p}/dt$ , one finds the continuity equation in pressure coordinates with additional terms due to the divergence of the precipitation mass flux and the water vapor diffusion flux. This aspect was discussed in Trenberth (1991) and Lackmann and Yablonsky (2004).

#### 4. Numerical examples for the field of $w_s$

In WH03, simple estimates were given to illustrate the order of magnitude of the vertical velocity  $w_s$  for typical values of evaporation and precipitation rates. The full proof of the significance of the accurate representation of the lower boundary conditions for vertical velocity can be given only from sensitivity studies with a numerical prediction model for the atmosphere that makes use of the exact formulation of the mass budget. Since such a model is not yet available, it is only possible to diagnose the barycentric velocity at the surface from simulation results of numerical prediction models, notwithstanding that they use the simplified condition  $w_s = 0$  during the integration cycle and therefore do not account for any interactions between the proper boundary velocity and the evolution of the field variables.

In the following case studies,  $w_s$  is estimated for two extreme weather situations. These are 1) a polar cold air outbreak with low atmospheric water concentrations, and 2) a tropical cyclone with high atmospheric water concentrations. In doing this we evaluate (22) with the momentary values of the surface fluxes of water vapor and precipitation, and due to the model condition  $w_s = 0$  we can broadly refer to them as evaporation rate and precipitation rate. The denominator in (22) is approximated by total air density minus water vapor density, calculated from surface conditions.

We use the operational mesoscale weather prediction model Lokal-Modell (LM) of the Deutscher Wetterdienst. The LM is a nonhydrostatic model, and the reference velocity is barycentric. The effects of subgrid-scale processes are represented in parameterized form. For instance, cloud microphysical processes are taken into account by a scheme of Kessler type, which additionally allows for the ice phase in the forms of cloud ice and precipitating ice. The simulations are run with a horizontal grid spacing of approximately 7 km and with 35 unequally spaced vertical levels of a hybrid coordinate. The model version is V2.19 for the cold air outbreak case. The model version V2.12 is used for the tropical cyclone case with a cloud microphysics param-

eterization scheme considering ice only in the form of precipitating ice. For model documentation see Doms and Schättler (1999, 2002). For applications of the model to an Arctic cold air outbreak see Wacker et al. (2005), and to a tropical cyclone see Frisius (2004).

##### a. Case study for a cold air outbreak

The first case considered is the northern flow across the marginal sea ice zone in the Fram Strait region between Greenland and Svalbard from 4 to 5 April 1998. Initial and boundary data are taken from the Europa-Modell (EM) analysis and forecast, respectively, and are interpolated from the EM grid to the LM grid. The EM was the operational weather forecast model of the DWD during the 1990s. The simulation is initialized for 0000 UTC 4 April 1998, and boundary data are updated every 6 h. For details of simulations of this case see Wacker et al. (2005); the model setup used here is similar to their control run, except the convection parameterization is switched on.

Figure 1 shows the horizontal distributions of near-surface wind and temperature, precipitation and evaporation rates, and the vertical velocity  $w_s$  at the surface. During this cold air outbreak episode very cold air over the pack ice propagated southward. When the cold air flows across the ice margin over the comparatively warm open water, it is strongly heated from below. A cloud-topped convective boundary layer forms with a typical boundary layer depth rising from several hundreds of meters close to the ice edge to about 1000 m at a distance of 300 km downstream from the ice edge. This weather situation persisted for several days.

The horizontal distribution of the simulated momentary precipitation rate, valid at 1200 UTC, is shown in Fig. 1b in units of millimeters of water per 6 h. The simulated clouds in the convective boundary layer downstream of the ice edge produce light drizzle. The precipitation rates correspond to about 1 mm per 6 h. In the southeastern part of the model domain precipitation rates locally exceed 2 mm per 6 h. Over Svalbard and Norway, precipitation seems to be effected by orography.

The simulated momentary rate of surface evaporation from the ocean into the atmosphere is given in Fig. 1c in the same units as the precipitation rates; that is, in millimeters of water per 6 h. The strongest evaporation rates of nearly 2 mm per 6 h are found close to the ice edge due to the large difference in the water vapor concentration within the cold air and at the sea surface, where water saturation is assumed.

The resulting  $w_s$  distribution, calculated from (22), is given in Fig. 1d. In the central region of the model domain over an ice-free ocean, evaporation exceeds

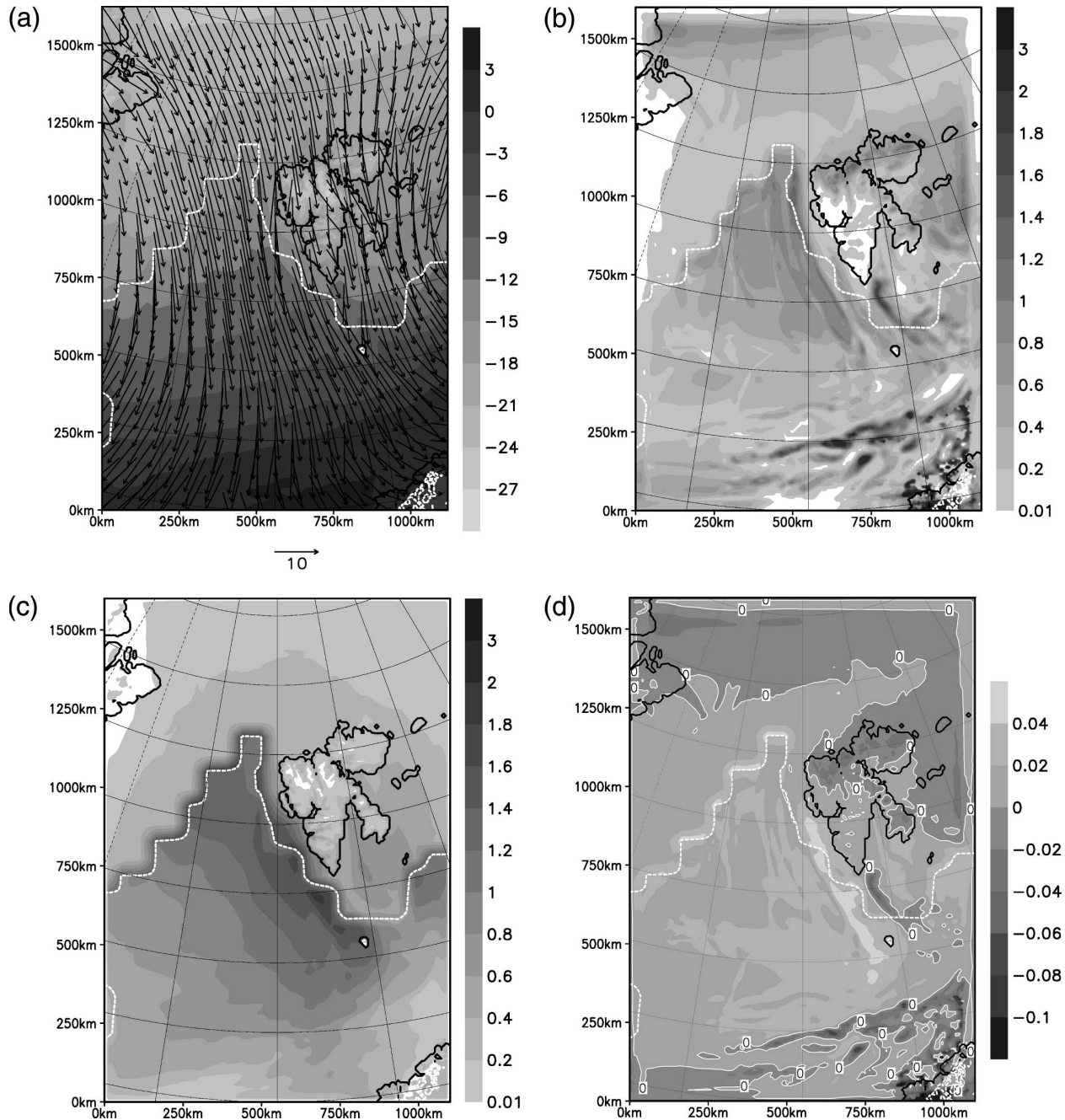


FIG. 1. Horizontal distributions for the cold air outbreak simulation, valid at 12-h simulation time starting at 0000 UTC 4 Apr 1998. Dashed white lines mark sea ice edge. (a) Horizontal wind field for the lowest model level (approximately 30 m above surface). Every eighth horizontal wind vector is plotted. Arrow length indicates wind speed; see scaling arrow for 10 m s<sup>-1</sup> wind speed. Shadings indicate near-surface temperature (°C). (b) Precipitation rate given in units mm water per 6 h. (c) Evaporation rate, given in the same unit (mm within 6 h) as the precipitation rates. (d) Surface vertical velocity  $w_s$  (in mm s<sup>-1</sup>) according to (22). Thin white line marks  $w_s = 0$ .

precipitation, and this net mass transfer into the atmosphere causes an upward barycentric velocity  $w_s$  at the surface. The local precipitation cells in the south east mean a net mass loss from the atmosphere, related to

negative values of  $w_s$ . Nevertheless, the vertical velocity remains weak with values ranging only between about 0.04 and  $-0.08$  mm s<sup>-1</sup>. The net mass transport into or out of the atmosphere contributes to the surface pres-

sure tendency, see Eq. (23); the contributions range between  $4 \times 10^{-4}$  and  $-8 \times 10^{-4} \text{ Pa s}^{-1}$ , corresponding to no more than about 0.7 and  $-1.4 \text{ hPa}$  within 48 h, if the meteorological situation holds more or less unchanged.

### b. Case study for a hurricane

Hurricanes are intense vortical storms on the meso-scale that develop over the tropical oceans in regions of very warm surface water, typically having temperatures of at least  $26^\circ\text{C}$  (Holton 1992). Their development requires a strong moisture supply to provide sufficient heat input in the atmosphere due to release of latent heat. Much of the moisture input is due to evaporation from the warm ocean, and the high condensation rate in the cumulus towers of the hurricane lead to heavy precipitation. Thus, such a hurricane situation is connected with large water mass fluxes at the ocean surface, and we expect accordingly a much larger value of the surface vertical velocity  $w_s$ , due to the local mass imbalance than in the previous case of a polar weather situation.

In the following we discuss a mature tropical cyclone as simulated with LM using artificial initial and boundary conditions. Initially, an axisymmetric cyclone lies at the center of the model domain. The initial cyclone has a radius of 150 km, and the central sea level pressure is 5 hPa below its ambient value. The tropospheric lapse rate amounts to  $0.65 \text{ K (100 m)}^{-1}$  and the relative humidity is 70% everywhere. The effects of spherical geometry are neglected and the Coriolis parameter takes the constant value  $f = 0.729 \times 10^{-4} \text{ s}^{-1}$ . A sea surface temperature of  $28^\circ\text{C}$  is assumed. The parameterization of moist convective processes is not switched on; instead it is assumed that the turbulence scheme adequately accounts for the subgrid-scale transport. More details of this simulation are given by Frisius (2004).

Figure 2 displays a snapshot of sea level pressure, wind at 10-m height, vertically integrated cloud water content, precipitation and evaporation rates, and vertical velocity  $w_s$  at the surface, all valid at 108 h simulation time. The model develops hurricane force winds ( $>32.7 \text{ m s}^{-1}$ ) near the surface within 36 h and the sea level pressure drops below 950 hPa after 90 h. The maximum wind speeds occur near the open ring of enhanced cloud water content, and this region can be associated with the eyewall of the tropical cyclone. Another remarkable feature is the spiral band in the southern part of the tropical cyclone.

The momentary maximum precipitation rate exceeds  $500 \text{ mm (6 h)}^{-1}$  locally in the western part of the eyewall (see Fig. 2b). Enhanced precipitation also occurs at other locations, especially in the spiral band. The distribution of the evaporation rate is similar to that of the

surface wind speed field since evaporation increases with wind speed. Much lower peak values are found in evaporation than in precipitation rates (see Fig. 2c). Hence, near the eyewall and the spiral band we have a net loss of mass from the atmosphere, causing a downward barycentric velocity at the surface with values greater than  $w_s \approx -20 \text{ mm s}^{-1}$  (see Fig. 2d). The mass loss due to precipitation is equivalent, according to (23), to a surface pressure decrease of  $0.23 \text{ Pa s}^{-1}$  (corresponding to 49 hPa within 6 h). The 6-h average values of precipitation and evaporation rates certainly reveal weaker extrema, namely a contribution to pressure tendency of 22 hPa within 6 h, yet this is still a remarkable pressure drop. Although one can expect that the modification of the mass field will cause a circulation to smooth the gradients, it seems unlikely that such a drop in pressure should not affect the dynamic situation at all.

Outside of the central hurricane region, where hardly any precipitation falls, we have a net mass gain of the atmosphere due to evaporation and, hence, we find a comparatively weak upward motion at the surface of the order of less than  $1 \text{ mm s}^{-1}$ .

## 5. Discussion

In this study, we have reexamined the local mass balance equations of cloudy air together with the lower boundary condition for vertical velocity. This was carried out for a model of cloudy air, as is typically assumed in numerical weather prediction models or in climate models with water considered in the five categories water vapor, cloud water, cloud ice, rainwater, and precipitating ice or snow. The barycentric velocity of the total system was chosen to define the reference motion, because only with this precondition does the continuity equation for total mass in the form of (13) follow without internal sources and divergence of diffusion fluxes. It is found that, owing to the mass transport by evaporation and precipitation at the earth's surface (here taken to be flat), the vertical velocity  $w_s$  at the surface is proportional to the local difference in evaporation rate and rain plus snow rate, given in terms of either the total or the diffusive mass fluxes, see (21) and (22), respectively. Hence,  $w_s$  is zero only in the special situation that evaporation and precipitation balance exactly. This, however, is a rare situation.

At present, no complex atmospheric prediction model makes use of this correct boundary condition for  $w_s$ , although steps in this direction have been made by Lackmann and Yablonsky (2004) as well as Saito (1998). Therefore, we cannot investigate the effect of using the correct boundary condition in combination with its interaction with the atmospheric evolution. In-

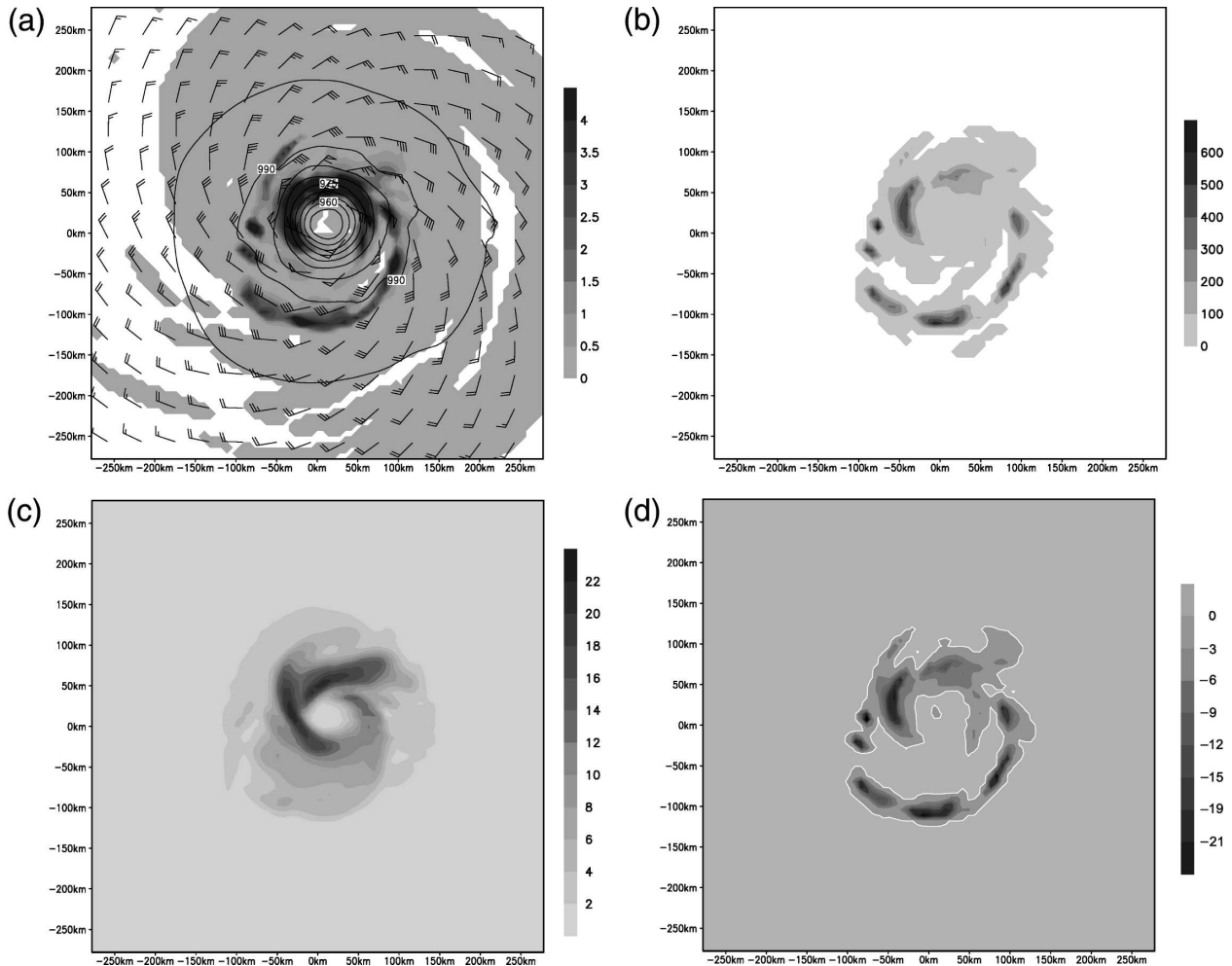


FIG. 2. Horizontal distributions for the hurricane simulation, valid at 108-h simulation time. (a) Sea level pressure (isolines, contour interval 5 hPa), 10-m wind (wind barbs, plotted for every sixth grid point; speed in knots) and vertically integrated cloud water mass in  $\text{kg m}^{-2}$  (shadings). (b) Precipitation rate given in units mm water per 6 h. (c) Evaporation rate, given in the same unit (mm within 6 h) as the precipitation rates. (d) Surface vertical velocity  $w_s$  (in  $\text{mm s}^{-1}$ ) according to (22). Thin white line marks  $w_s = 0$ .

stead, we can only diagnose a vertical velocity  $w_s$  from model results of evaporation and precipitation rates. This has been carried out for two weather situations which are simulated with the nonhydrostatic numerical weather prediction model LM. For the situation of the polar cold air outbreak,  $w_s$  turns out to be weak as expected for a cold atmosphere, characterized by low concentrations of water vapor and condensate. However, for the tropical cyclone case, with precipitation rates up to more than  $0.023 \text{ mm s}^{-1}$  (corresponding to 500 mm within 6 h), the vertical velocity can be stronger than  $-20 \text{ mm s}^{-1}$  at the surface due to the net local mass loss. This loss corresponds to a drop in hydrostatic surface pressure of more than  $0.23 \text{ Pa s}^{-1}$  (corresponding to 49 hPa within 6 h). It seems unlikely that such a pressure change should not influence the dynamics,

even though feedback mechanisms may dampen the effect. Indeed, Lackmann and Yablonsky (2004) found from their modeling study that the mass sink due to precipitation exerts a nonnegligible influence on the dynamics of a tropical cyclone.

While in most atmospheric situations the implication of the choice of the reference velocity should be negligible due to the abundance of dry air, matters may become different close to the surface, where dry air vertical velocity tends to zero; it is then necessary to choose a matching combination of the reference velocity and its boundary condition to account for the mass fluxes across the boundaries of the open system. The barycentric reference velocity provides advantages for the field balance equations. The total mass continuity equation exactly follows in the form of (13) or in pres-

sure coordinates in the form of (25), while for other reference velocities additional contributions should be included to account for diffusion and phase change effects.

The barycentric velocity is determined from the momentum equation for the total system air. Since the internal momentum transfers do not modify the total momentum, no additional closure assumptions are required as in the case of the dry air or gas mixture momentum equations. The pressure tensor in (24), the diffusive mass fluxes in (9), and other irreversible fluxes are accessible only in the barycentric reference frame by parameterization equations provided by the theory of irreversible processes (Herbert 1973). We conclude that the use of the barycentric velocity in the field balance equations should be favored, in combination with the proper boundary condition (21) or (22) for the vertical velocity, to account for the net mass transfer across the earth's surface. The latter effect should not be neglected in numerical weather prediction or climate models because of the sometimes significant impacts as in the hurricane case and because evaporation and precipitation rates differ systematically for most places on a climatological time scale.

*Acknowledgments.* We gratefully acknowledge the comprehensive and helpful work of the reviewers. Thanks are also to the staff of DWD's Business Area "Research and Development" for providing LM and substantial support. One of us (TF) thanks the DKRZ (Deutsches Klimarechenzentrum) for the use of their high performance computer on which parts of the numerical calculations have been done. We particularly thank Dr. Jill Schwarz, who helped us with the language of this paper.

#### REFERENCES

- Andreas, E. L., 2004: Spray stress revisited. *J. Phys. Oceanogr.*, **34**, 1429–1440.
- Bannon, P., 2002: Theoretical foundations for models of moist convection. *J. Atmos. Sci.*, **59**, 1967–1982.
- Doms, G., and F. Herbert, 1985: Fluid- und Mikrodynamik in numerischen Modellen konvektiver Wolken. Berichte des Instituts für Meteorologie und Geophysik der Universität Frankfurt am Main Rep. 62, 378 pp.
- , and U. Schättler, 1999: The nonhydrostatic limited-area model LM (Lokal-Modell) of DWD. Part I: Scientific documentation. Deutscher Wetterdienst (German Weather Service), 169 pp. [Available online at <http://cosmo-model.cscs.ch/public/documentationVer1.htm>.]
- , and —, 2002: A description of the nonhydrostatic regional model LM. Part I: Dynamics and numerics. Deutscher Wetterdienst (German Weather Service). [Available online at <http://cosmo-model.cscs.ch/public/documentation.htm#p1>.]
- Frisius, T., 2004: Numerical simulation of tropical cyclogenesis with the Lokal-Modell. *COSMO Newsletter*, No. 4, 189–196. [Available online at <http://cosmo-model.cscs.ch/public/newsLetters.htm>.]
- Gyarmati, I., 1970: *Non-equilibrium Thermodynamics*. Springer, 184 pp.
- Haase, R., 1990: *Thermodynamics of Irreversible Processes*. Dover Publications, 513 pp.
- Herbert, F., 1973: Irreversible Prozesse in der Atmosphäre; Teil 2. *Contrib. Atmos. Phys.*, **46**, 262–288.
- , 1983: PRIGOGINE's diffusion theorem and its application to atmospheric transfer processes, Part 2: Invariance properties and Fick type diffusion laws. *Contrib. Atmos. Phys.*, **56**, 480–494.
- Hesselberg, T., 1926: Die Gesetze der ausgeglichenen Bewegungen. *Beitr. Phys. Freien Atmos.*, **12**, 141–160.
- Holton, J. R., 1992: *An Introduction to Dynamic Meteorology*. Academic Press, 511 pp.
- Lackmann, G. M., and R. M. Yablonsky, 2004: The importance of the precipitation mass sink in tropical cyclones and other heavily precipitating systems. *J. Atmos. Sci.*, **61**, 1674–1692.
- Ooyama, K. V., 2001: A dynamic and thermodynamic foundation for modeling the moist atmosphere with parameterized microphysics. *J. Atmos. Sci.*, **58**, 2073–2103.
- Rogers, R. R., and M. K. Yau, 1989: *A Short Course in Cloud Physics*. Pergamon Press, 293 pp.
- Saito, K., 1998: Recent modification of the MRI-NHM. CAS/JSC WGNRE Research Activities in Atmospheric and Oceanic Modelling, Rep. 27, WMO-TD 865, 544–545.
- Satoh, M., 2003: Conservative scheme for a compressible nonhydrostatic model with moist processes. *Mon. Wea. Rev.*, **131**, 1033–1050.
- Schubert, W. H., S. A. Hausman, M. Garcia, K. V. Ooyama, and H.-C. Kuo, 2001: Potential vorticity in a moist atmosphere. *J. Atmos. Sci.*, **58**, 3148–3157.
- Stappeler, J., G. Doms, U. Schättler, H. W. Bitzer, A. Gassmann, U. Damrath, and G. Gregoric, 2003: Meso-gamma forecasts using the nonhydrostatic model LM. *Meteor. Atmos. Phys.*, **82**, 75–96.
- Stull, R. B., 1994: *An Introduction to Boundary Layer Meteorology*. Kluwer Academic, 666 pp.
- Trenberth, K. E., 1991: Climate diagnostics from global analyses: Conservation of mass in ECMWF analyses. *J. Climate*, **4**, 707–722.
- , J. W. Hurrell, and A. Solomon, 1995: Conservation of mass in three dimensions in global analyses. *J. Climate*, **8**, 692–708.
- Wacker, U., and F. Herbert, 2003: Continuity equations as expressions for local balances of masses in cloudy air. *Tellus*, **55A**, 247–254.
- , K. V. J. Potty, C. Lüpkes, J. Hartmann, and M. Raschendorfer, 2005: A case study on a polar cold air outbreak over Fram Strait using a mesoscale weather prediction model. *Bound.-Layer Meteor.*, **117**, 301–306.